Original Article
The PPAR signaling pathway as a potential biomarker for the diagnosis of breast cancer

Hengyu Wang, Yuqin Yang, Qing Luo, Minfeng Liu, Can Luo, Jianyu Dong, Jingyun Guo, Changsheng Ye

Department of Breast Surgery, Nanfang Hospital, Southern Medical University, Guangzhou, Guangdong Province, P. R. China

Abstract: Several previous studies have investigated the association between the peroxisome proliferator-activated receptor (PPAR) signal pathway and cancer risk; however, the results of these studies were inconsistent, and the role of the PPAR signaling pathway in cancer remains unclear. Therefore, the aim of this study was to further investigate the association between the PPAR signaling pathway and breast cancer risk. RNA-Seq expression data were derived from a breast cancer cohort of the Gene Expression Omnibus (GEO) dataset. A two-way hierarchical clustering analysis (HCA), a support vector machine (SVM) classifier, and a protein-protein interaction (PPI) network were built in the training dataset (GSE42568) using the twenty-one differentially expressed genes (DEGs) which were annotated into the PPAR signaling pathway. The accuracy of the candidate informative DEGs using the training dataset (GSE42568) in risk-stratifying samples was 72.73%, and the accuracy of the SVM classifier was 97.52%. The predictive ability of the validation datasets, GSE29431 and GSE21422, achieved reliable outcomes, with the risk-stratifying samples at 96.97% and 94.74%, respectively, from the two-way HCA. The accuracy yields were 92.42% and 94.74%, respectively, using the SVM classifier. A PPI analysis showed that the twenty-one DEGs formed a retinoid X receptor alpha (RXRA)-centric world with 14 nodes. Collectively, the twenty-one informative genes of the PPAR signaling pathway may represent the key genes associated with the occurrence of breast cancer. Our results provide the primary information and basic knowledge necessary to better understand the mechanisms of cancer pathogenesis.

Keywords: Breast cancer, gene expression omnibus datasets, peroxisome proliferator activated receptors signaling pathway, SVM classifier, two-way hierarchical clustering analysis

Introduction

Breast cancer (BC) is a common cancer among females in both developed and developing countries [1], with the risk of developing BC known to be influenced by both genetic and environmental factors. A total of 1.7 million new BC cases have been identified since 2012, with over 500,000 related deaths [2]. As BC cases continue to rise annually, corresponding to high mortality rates [3, 4], the association between potential environmental and genetic factors and BC risk needs to be further investigated. Recent studies have highlighted several genetic factors that appear to correlate with BC risk [5-7], including metabolism-related genetic variations [8].

Peroxisome proliferator-activated receptors (PPARs) comprise a cluster of nuclear transcription factors that are members of the nuclear

hormone receptor super-family. They possess important functions in cellular differentiation and the regulation of carbohydrates and lipid metabolism [9]. Accordingly, polymorphisms in these receptors are assumed to affect the pathology of cancers and other diseases. Three PPAR subtypes, namely, PPAR alpha (PPARA), PPAR delta/PPAR beta (PPARD/PPARB), and PPAR gamma (PPARG), have been found to be dynamically regulated at multiple molecular levels. Endogenous PPARA ligands include palmitic acid, arachidonic acid, and stearic acid. In addition, other known ligands include compounds such as fenofibrate, bezafibrate, and non-steroidal anti-inflammatory drugs [10, 11]. Thus far, genetic variants of PPARA have been related to lipoprotein levels [12], cardiovascular disease [13], obesity [14], and type 2 diabetes [15]. These conditions arise through etiologic mechanisms that may also be relevant to breast carcinogenesis, including inflammation and

insulin resistance. Although the biology and epidemiology of PPARA suggest that this receptor may also play a role in BC, limited data exist on the possible link between PPARA and BC.

PPARG plays a pivotal role in regulating adipocyte differentiation, glucose and lipid homeostasis, and intracellular insulin-signaling events [16]. In addition, PPARG appears to have a contradictory role in tumorigenicity. Indeed, several studies have demonstrated the tumorigenic role of PPARG in a variety of cancers such as bladder tumors, renal pelvic tumors, hemangioma, lipoma, skin fibrosarcoma, mammary adenocarcinoma, and hepatic tumors. The tumorigenicity of PPARs has not been fully recognized; however, recent studies have suggested various mechanisms for this reported effect. In contrast, the anti-tumorigenicity of PPARG agonists through other hypothesized mechanisms, as well as the downregulation of PPARG in some human cancers, has been reported [17-27]. Moreover, the activation of PPARG by its ligands can suppress the growth of tumor cells in liver, pancreatic, biliary, oral, esophageal, gastric, and colorectal tumors, suggesting that PPARG ligands may be a possible anticancer factor in PPARG-expressing tumors [28].

For complete activation, PPARs must heterodimerize with retinoid X receptors (RXR) to form a PPAR/RXR complex. This complex then binds to a specific DNA sequence, termed the PPAR-response element, in a given target gene [29]. RXRA is a nuclear receptor that regulates transcription, both as a homodimer and an obligate heterodimerization partner for 14 other nuclear receptors, including PPARA, PPARD, and PPARG [30].

Bioinformatics is an effective tool for collecting, classifying, and analyzing biological datasets, including gene expression microarray datasets [31, 32]. In fact, gene expression analysis by bioinformatics methods has been widely employed in genomics and biomedical research, broadening insights into the molecular mechanisms underlying human biology and disease [33]. Data mining of the available microarray datasets could assist scientists to bridge the research gap and to carry out more efficient experiments.

In this study, we analyzed public microarray data using a two-way hierarchical clustering analysis and a support vector machine (SVM) classifier in order to clarify potential associations between the PPAR signaling pathway and BC. Differentially expressed genes (DEGs) were first identified between the normal and tumor groups. From these DEGs, optimal informative genes were extracted using the DEGs annotated into the PPAR signal pathway. Candidate genes were then subjected to build a SVM classifier; the predictive capability of the candidate informative genes was then verified using two independent datasets. These informative genes were also utilized to construct protein-protein networks. Finally, we attempted to identify PPAR signal pathway-related genes to gain insight into the pathogenesis of BC.

Materials and methods

Data source

Two mRNA-seq expression datasets were accessed from the Gene Expression Omnibus data portal (https://www.ncbi.nlm.nih.gov/geo/). The GSE42568 dataset was used as a training set, which included 104 primary breast samples and 17 normal control samples. The GSE-29431 and GSE21422 datasets were used as validation sets and consisted of 54 primary melanoma samples and 12 normal control samples and 14 primary melanoma samples and 5 normal control samples, respectively. The three mRNA expression datasets were assessed using GPL570 Platform. All microarray data were called using the GC robust multichip average method [34] and quantile normalized using the "affy" Bioconductor package by contributor.

Data preprocessing and differentially expressed genes (DEG) screening

Annotations to the probes were performed; probes that were not matched to the gene symbol were excluded. The average expression values were taken if different probes mapped to the same gene. DEGs in patients with BC versus those in healthy matched controls were analyzed using the DESeq package (version 3.10.3) of Bioconductor. A strict cutoff threshold was used and set to $P<0.05$ and fold change ≥ 2.0.

Predictive capacity in proposed HCA and SVM classifier model

The DEGs that were annotated into the PPAR pathway were selected for further analysis.
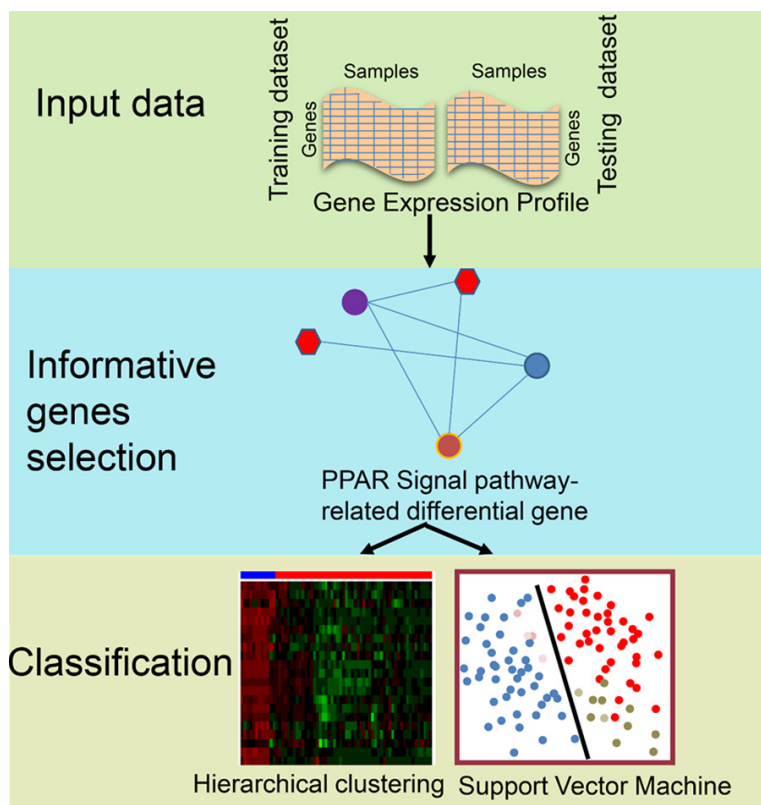
Figure 1. The procedure of the proposed method. The workflow consisted of three key parts: gene expression data processing, screening PPAR signal pathway-related differential genes, and distinguishing the disease status of the samples.

Two-way HCA was performed on the expression values of genes that were significantly overlapping using the heatmap2 package (21) in R, and the distance was under default value.

A SVM classifier was constructed using the support vector classification function in sklearn in the svm package of Python (version 3), with the linear Kernel function (C=0.3) and a 3-fold cross-validation. In addition, the random seed was held at 100 to shuffle the training set. The capacity of classification were evaluated based on six metrics, including the accuracy, sensitivity, specificity, positive predictive value (PPV), negative predictive value (NPV), and area under the receiver operating curve (AUC).

Verification of the classification model using other two independent dataset

Two-way HCA and the SVM classifier, based on the candidate informative genes, were conducted sequentially to further verify classifica-

tion reliability by computing other two independent dataset as the test set.

Construction of mRNA-mRNA networks

The Search Tool for the Retrieval of Interacting Genes/Proteins (STRING; http://www. STRING database.org/) [35] is a gene or protein analysis tool designed to provide a critical assessment and integration of protein-protein interactions (PPIs). In this study, overlapping genes were mapped into the STRING database for PPI analysis and PPI scores >0.4 were selected as significant [36, 37]. A PPI network was then constructed using Cytoscape software (version 3.5.1) [38], and the degree was used for stating the role of the protein nodes in the network. Specifically, the greater the degree, the more important the nodes were in the network. In PPIs, genes closely associated with other genes were identified with degrees ≥10 [37, 39].

Results

HCA and SVM classifier for distinguishing disease status

To examine the PPAR signal pathway on BC risk, we used two independent methods, namely, HCA and SVM classifier. Using these methods, we identified shared DEGs in the PPAR signal pathway. Using HCA, the association between the expression pattern of candidate genes and the disease status of the samples were identified with the Euclidean method. SVM classifier discrimination between cancer patients and healthy samples was based on a hyperplane to maximize the distance between two samples on different sides of the plane, which were the closest samples to the plane in each category, respectively. The general workflow were showed in **Figure 1**.
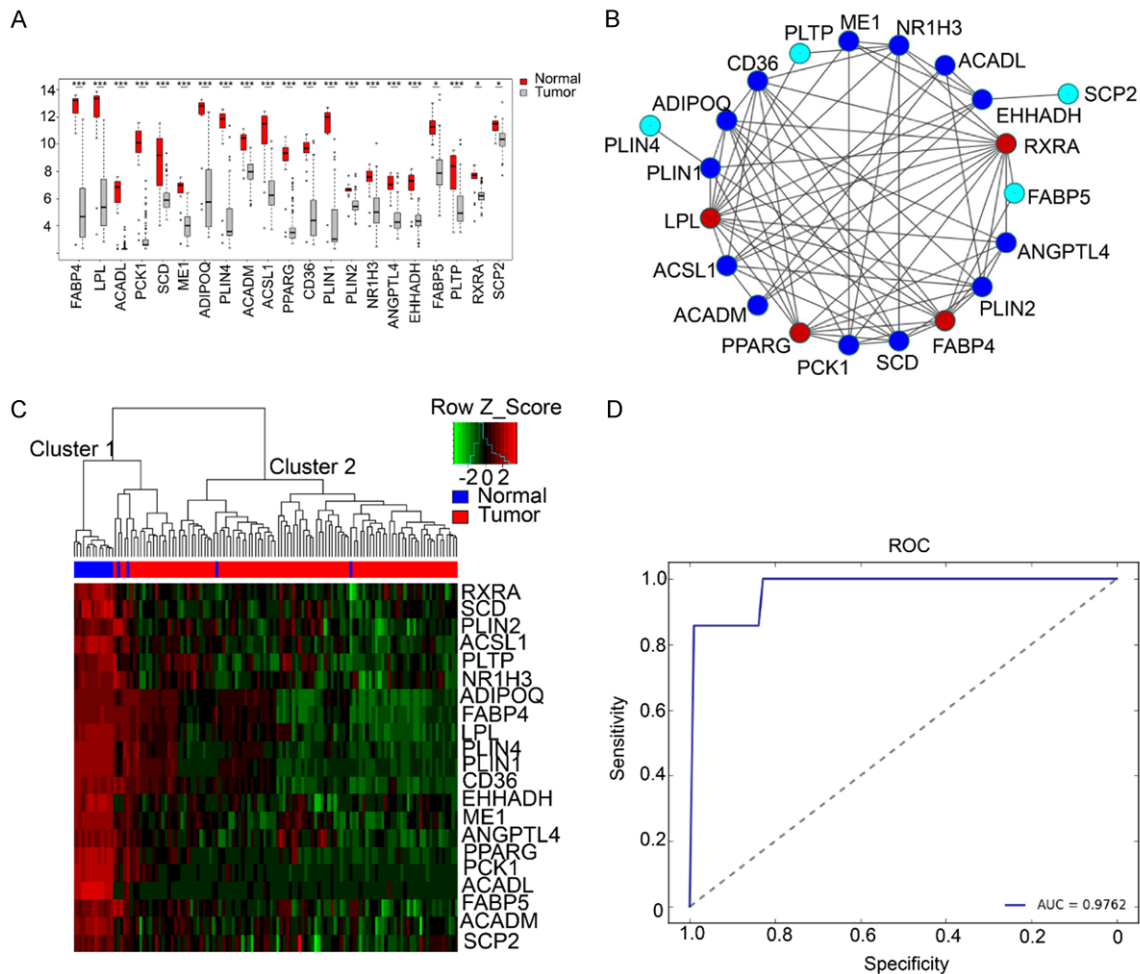
Figure 2. Analysis of twenty-one candidate signature genes in the training cohort (GSE42568). A. Expression distribution of twenty-one differentially expressed genes in breast cancer patients and normal samples in the discovery cohort analyzed by microarray. The red color represents the normal group, whereas grey represents the tumor group. The log2 ratio of expression (normal/tumor) is displayed on the *y*-axis, and the gene category is displayed on the *x*-axis. B. PPI network. The color depth represents the weight of genes in the network; nodes less than 3 are in sky blue, with a gradual change from sky blue to dark blue indicating nodes greater than 3 and less than 10. Red indicates the hub genes, with nodes greater than 10. C. Heatmap showing the gene expression profile of twenty-one candidate PPAR pathway-related genes based on hierarchical clustering. The blue color represents the normal group, whereas the red color represents the tumor group. Upregulated and downregulated genes are indicated by red and green, respectively. D. Receiver operating characteristic (ROC) analysis of the SVM classifier based on the twenty-one candidate signature in the training set. All samples in the training set were classified into the tumor group and normal match group via the SVM classifier; tumor samples were set as the positive group, whereas the normal samples were set as the negative group.

Identification of selected informative genes

A total of 1833 DEGs were identified between normal and control samples using R software. Of these, 684 were upregulated, whereas 1149 were downregulated. Twenty-one candidate informative genes of the PPAR pathway were selected for further analysis. These included FABP4, LPL, ACADL, PCK1, SCD, ME1, ADIPOQ, PLIN4, ACADM, ACSL1, PPARG, CD36, PLIN1, PLIN2, NR1H3, ANGPTL4, EHHADH, FABP5,

PLTP, RXRA, and SCP2. The distribution of the expression levels of the twenty-one candidate PPAR pathway-associated genes was shown in **Figure 2A**, with the detailed information provided in **Table 1**.

PPI network analysis

In view of the controversy between PPARs and cancer, the twenty-one candidate associated genes were selected to perform further analy-

Table 1. Detail information of twenty-one candidate signature genes

Status	Gene name	log$_2$FC	*p*-value	p-adjust
Downregulated	FABP4	-4.54	2.32E-55	5.46E-51
	LPL	-5.43	1.08E-30	1.02E-27
	ACADL	-4.33	4.56E-15	5.42E-13
	PCK1	-6.62	4.76E-27	2.67E-24
	SCD	-3.5	1.29E-11	9.75E-10
	ME1	-3.89	3.31E-24	1.26E-21
	ADIPOQ	-4.3	4.59E-36	9.00E-33
	PLIN4	-5.3	3.24E-28	2.24E-25
	ACADM	-2.18	4.72E-12	3.86E-10
	ACSL1	-3.78	6.27E-29	4.76E-26
	PPARG	-4.98	4.24E-24	1.56E-21
	CD36	-4.67	6.61E-26	3.11E-23
	PLIN1	-5.99	1.01E-38	2.98E-35
	PLIN2	-1.89	2.50E-05	5.97E-04
	NR1H3	-1.89	3.64E-05	8.28E-04
	ANGPTL4	-2.09	4.21E-08	1.76E-06
	EHHADH	-2.71	4.45E-09	2.29E-07
	FABP5	-2.19	3.19E-04	5.66E-03
	PLTP	-1.95	4.13E-05	9.20E-04
	RXRA	-1.92	5.22E-04	8.60E-03
	SCP2	-1.03	1.44E-04	2.84E-03

Table 2. Summary of clinical samples in the training and two test datasets

	Cancer	Healthy	Total
Cancer	86	2	88
Healthy	18	15	33
	104	17	121

Note: The row was the actual class, and the column was the predicted class (training dataset, GSE42568).

	Cancer	Healthy	Total
Cancer	54	2	56
Healthy	0	10	10
	54	12	66

Note: The row was the actual class, and the column was the predicted class (test dataset, GSE29431).

	Cancer	Healthy	Total
Cancer	14	1	15
Healthy	0	4	4
	14	5	19

Note: The row was the actual class, and the column was the predicted class (test dataset, GSE21422).

sis. This PPI network was visualized using Cytoscape. Hub genes with a degree of interaction >10 were defined as those that strongly interacted with other candidate genes, including RXRA, LPL, FABP4, and PPARG (**Figure 2B**). These hub genes may represent key genes affected by the PPAR signal pathway that were associated with BC.

HCA of candidate mRNAs

A total of twenty-one candidate PPAR pathway-associated logarithmic expression values were subjected to HCA using the training set. As shown in **Figure 2**. As the result showed that all samples were distinctly subdivided into two clusters. The accuracy was 72.73% (88/121) and more specifically, 15 out of the 17 normal samples were incorporate into individual cluster and 86 out of the 104 tumor samples were classified into the other cluster (**Figure 2C**; **Table 2**).

Assessment on the training dataset using the SVM classifier model

To further confirm whether the candidate signature genes can discriminate between the two types of samples, an SVM classifier model was proposed on the basis of their expression values and achieved reliable result with the accuracy of 97.52%, a sensitivity of 99.05%, a specificity of 83.33%, a PPV of 97.25%, a NPV of 94.44%, and AUC of 97.62% (**Figure 2D**; **Table 3**).

Validation of the classification model in GSE29431 cohort

The performance of two-way HCA and the SVM classifier based on the twenty-one candidate signature genes was verified using the testing datasets. The results of two-way HCA indicated that all the samples in the validation dataset were stratified into two groups. The accuracy was thus determined to be 96.97% (64/66), only 2 normal samples incorrectly clustered into the tumor group and all tumor samples were extremely accurate classified into the corresponding group (**Figure 3A**; **Table 2**).

Likewise, the SVM model could correctly distinguish the tumor sample and normal samples attaining high accuracy (92.42%), and AUC, the sensitivity, specificity, PPV and NPV reaching 88.27%, 94.44%, 83.33%, 96.23%, 76.92%, respectively (**Figure 3B**; **Table 3**).

Table 3. Performance of twenty-one candidate signature genes in SVM classifier

Metrics	Training dataset	Test datasets	
	GSE42568	GSE29431	GSE21422
Accurancy	97.52%	92.42%	94.74%
Sensitivity	99.05%	94.44%	100.00%
Specificity	83.33%	83.33%	80.00%
PPV	97.25%	96.23%	93.33%
NPV	94.44%	76.92%	100.00%
AUC	97.62%	88.27%	95.71%

Note: The tumor samples were set as positive group, while the normal sample as negative group.

Further validation in the GSE21422 cohort

Further validation of the predictive value of the candidate genes in the diagnosis of BC was conducted using another independent validation cohort. HCA of all samples (*n*=19) revealed clear distinctions between BC patients and healthy samples. Samples were classified into cluster 1 and cluster 2, and achieved a prediction accuracy of 94.74% with one normal sample incorrectly clustered into the tumor group (18/19) (**Figure 3C**). The SVM-based candidate gene risk classifier performed remarkably well. The accuracy was 94.74%, with an AUC of 95.71%, a sensitivity of 100.00%, specificity of 80.00%, PPV of 93.33%, and a NPV of 100.00% (**Figure 3D**; **Table 3**). In total, these results confirmed the twenty-one candidate signature genes can reliably discriminate the normal sample from controls in BC.

Discussion

Many studies have shown that BC is a metabolic disease [40, 41]. For example, the glutamate-to-glutamine ratio and aerobic glycolysis have been proposed as biomarkers of ER and Her2 status, respectively [42, 43]. PPARs are key transcriptional factors that catalyze and coordinate a variety of biochemical events in order to achieve energy homeostasis associated with many types of cancer, including hepatocellular carcinoma [44], lung adenocarcinoma [45], squamous cell carcinoma of the head and neck [46], bladder cancer [47], and skin carcinoma [48]. However, the association between the PPAR pathway and cancer risk remains controversial, and a prospective analysis is essential to determine any potential relationships.

Currently, several advanced biological techniques, including gene array and high-through-put sequencing, have been identified as ideal approaches for assessing the mechanisms of development and the immune responses to various diseases. In this study, a comprehensive bioinformatics analysis of several gene array datasets was applied to determine DEGs in BC and their associated pathways. A total of 1833 DEGs were identified to be associated with BC, including 684 upregulated DEGs and 1149 downregulated DEGs. Twenty-one candidate downregulated signature genes were then annotated into the PPAR signal pathway. Key selected downregulated DEGs were further used to investigate the PPI network analysis. Our results demonstrated that the RXRA and FABP4 genes presented with substantially more "weight" than the other genes in the interaction network.

Recent studies have shown that PPARG inhibits cellular proliferation and induces apoptosis through the upregulation of phosphatase and tensin homolog (PTEN), the downregulation of survivin, the downregulation of the X-linked inhibitor of apoptosis (XIAP), suppression of NF-κB and glycogen synthase kinase (GSK)-3β, upregulation of cyclin-dependent kinase (CDK) inhibitors, downregulation of CDK and cyclin D1, downregulation of prostaglandin-endoperoxide synthase 2 (PTGS2), upregulation of Kruppel-Like Factor 4 (KLF4), upregulation of Bax, downregulation of Bcl-2, and inhibition of telomerase activity and human telomerase reverse transcriptase (hTERT) expression through modulation of the Myc/Mad/Max network [49]. However, complete activation is dependent on heterodimerization with RXR, thus forming a PPARG/RXRA complex. We therefore speculated that the downregulated expression level of the PPARG/RXRA complex induces cellular proliferation and blocks apoptosis, resulting in BC.

To further investigate the association between the PPAR pathway and BC risk, the twenty-one candidate signature genes were selected for two-way HCA and to train the SVM classifier. 17 normal samples versus 104 tumor samples were used in the trial. The resulting outcomes showed that the accuracy of the informative genes was 72.73%. The classification capability of the signature genes was further verified using two independent datasets (GSE29431 and GSE21422) that included 12 normal samples versus 54 tumor samples, and 5 normal samples versus 14 tumor samples, respective-
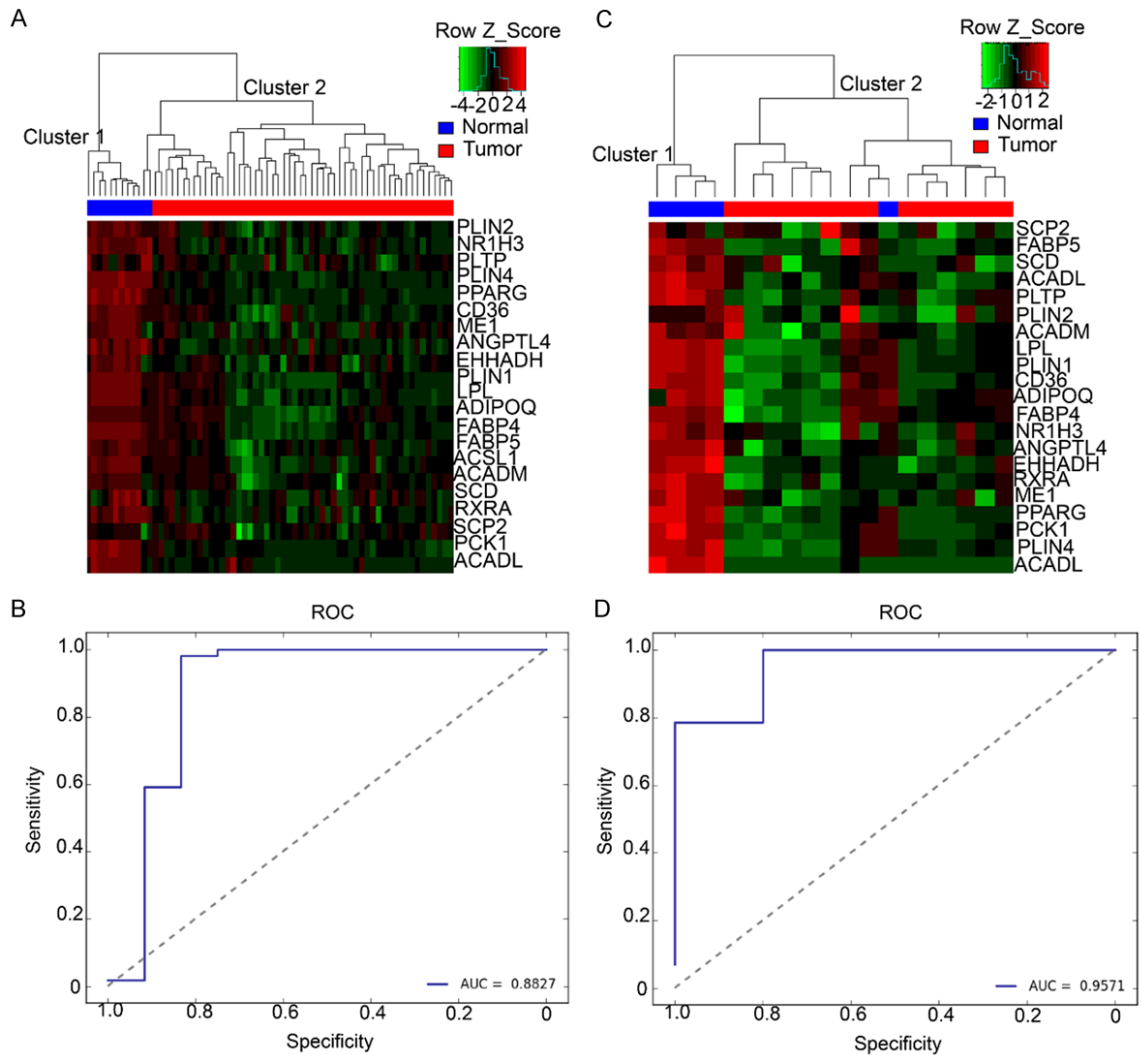
Figure 3. Performance of the two-way HCA and the support vector machine (SVM) classifier based on twenty-one candidate signature genes in the independent validation cohorts (GSE29431 and GSE21422). A. A heatmap of clustering analysis in the GSE29431 cohort. All samples were clustered into cluster 1 and cluster 2. B. ROC analysis of the SVM classifier in the GSE29431 cohort. All samples in the validation set were divided into the tumor group and normal group via the SVM classifier. C. The heatmap of HCA of all samples in the GSE21422 cohort. D. ROC analysis of the SVM-based twenty-one candidate signature genes in the GSE21422 cohort.

ly. Two-way HCA and SVM classifier analysis achieved consistent results, supporting our conclusion that these twenty-one candidate PPAR pathway-related genes exhibit a potential association between PPAR and BC risk. However, few reports exist regarding the involvement of these candidate genes in BC. Hence, further studies implicating the associations between the genes identified in this study and BC are warranted.

In conclusion, the present study identified twenty-one key DEGs in the progress of BC. Our results indicated that the four key genes, RXRA, LPL, FABP4, and PPARG, had a high degree of interaction, implying that they may co-function in the tumorigenesis of BC by participating in the regulation of the PPAR signaling pathway. However, further laboratory experiments are still required to confirm the exact association between these genes in order to clearly understand what correlation patterns exist among them. Collectively, the present study provided basic information, paving the road for future experimental research to investigate the mechanisms of BC development. Increasing knowl-

edge regarding the mechanisms of BC may lead to improved diagnostic efficacy, as well as the development of novel treatments.

Disclosure of conflict of interest

None.

Address correspondence to: Dr. Changsheng Ye, Department of Breast Surgery, Nanfang Hospital, Southern Medical University, 1838 Tonghe Road, Guangzhou 510515, Guangdong Province, P. R. China. Tel: +86-20-37089917; Fax: +86-20-3708-9917; E-mail: yechsh2006@126.com

References

[1] Cruwys C and Pushkin J. Breast density and impacts on health. Ecancermedicalscience 2017; 11: ed70.

[2] Ferlay J, Soerjomataram I, Dikshit R, Eser S, Mathers C, Rebelo M, Parkin D, Forman D and Bray F. Cancer incidence and mortality worldwide: sources, methods and major patterns in GLOBOCAN 2012. Int J Cancer 2015; 136: E359-386.

[3] WHO. World health statistics 2008. World Health Organization 2008.

[4] Murray CJ, Lopez AD; Organization WH. The global burden of disease: a comprehensive assessment of mortality and disability from diseases, injuries, and risk factors in 1990 and projected to 2020: summary. 1996.

[5] Guo H, Ming J, Liu C, Li Z, Zhang N, Cheng H, Wang W, Shi W, Shen N and Zhao Q. A common polymorphism near the ESR1 gene is associated with risk of breast cancer: evidence from a case-control study and a meta-analysis. PLoS One 2012; 7: e52445.

[6] Li LW and Xu L. Menopausal status modifies breast cancer risk associated with ESR1 PvuII and XbaI polymorphisms in Asian women: a HuGE review and meta-analysis. Asian Pac J Cancer Prev 2012; 13: 5105-5111.

[7] Yu L and Chen J. Association of MHTFR Ala222Val (rs1801133) polymorphism and breast cancer susceptibility: an update meta-analysis based on 51 research studies. Diagn Pathol 2012; 7: 171.

[8] Wu MH, Chu CH, Chou YC, Chou WY, Yang T, Hsu GC, Yu CP, Yu JC and Sun CA. Joint effect of peroxisome proliferator-activated receptor γ genetic polymorphisms and estrogen-related risk factors on breast cancer risk: results from a case-control study in Taiwan. Breast Cancer Res Treat 2011; 127: 777-784.

[9] Cho MC, Lee K, Paik SG and Yoon DY. Peroxisome proliferators-activated receptor (PPAR) modulators and metabolic disorders. PPAR Res 2008; 2008: 679137.

[10] Kota BP, Huang TH and Roufogalis BD. An overview on biological mechanisms of PPARs. Pharmacol Res 2005; 51: 85-94.

[11] van Raalte DH, Li M, Pritchard PH and Wasan KM. Peroxisome proliferator-activated receptor (PPAR)-α: a pharmacological target with a promising future. Pharm Res 2004; 21: 1531-1538.

[12] Tai E, Demissie S, Cupples L, Corella D, Wilson P, Schaefer E and Ordovas J. Association between the PPARA L162V polymorphism and plasma lipid levels: the framingham offspring study. Arterioscler Thromb Vasc Biol 2002; 22: 805-810.

[13] Balcerzyk A, Zak I and Krauze J. Synergistic effect between polymorphisms of PPARA and ABCA1 genes on the premature coronary artery disease. Acta Cardiol 2007; 62: 233-238.

[14] Evans D, Aberle J, Wendt D, Wolf A, Beisiegel U and Mann W. A polymorphism, L162V, in the peroxisome proliferator-activated receptor α (PPAR α) gene is associated with lower body mass index in patients with non-insulin-dependent diabetes mellitus. J Mol Med 2001; 79: 198-204.

[15] Flavell DM, Ireland H, Stephens JW, Hawe E, Acharya J, Mather H, Hurel SJ and Humphries SE. Peroxisome proliferator-activated receptor α gene variation influences age of onset and progression of type 2 diabetes. Diabetes 2005; 54: 582-586.

[16] Auwerx J. PPARγ, the ultimate thrifty gene. Diabetologia 1999; 42: 1033-1049.

[17] Zurlo D, Ziccardi P, Votino C, Colangelo T, Cerchia C, Dal Piaz F, Dallavalle S, Moricca S, Novellino E and Lavecchia A. The antiproliferative and proapoptotic effects of cladosporols A and B are related to their different binding mode as PPARγ ligands. Biochem Pharmacol 2016; 108: 22-35.

[18] Yin Y, Hou G, Li E, Wang Q and Kang J. PPAR Gamma agonists regulate tobacco smoke-induced toll like receptor 4 expression in alveolar macrophages. Respir Res 2014; 15: 28.

[19] Yang Y, Zhao LH, Huang B, Wang RY, Yuan SX, Tao QF, Xu Y, Sun HY, Lin C and Zhou WP. Pioglitazone, a PPARγ agonist, inhibits growth and invasion of human hepatocellular carcinoma via blockade of the rage signaling. Mol Carcinog 2015; 54: 1584-1595.

[20] Wu K, Yang Y, Liu D, Qi Y, Zhang C, Zhao J and Zhao S. Activation of PPARγ suppresses proliferation and induces apoptosis of esophageal cancer cells by inhibiting TLR4-dependent MAPK pathway. Oncotarget 2016; 7: 44572.

[21] Srivastava N, Kollipara RK, Singh DK, Sudderth J, Hu Z, Nguyen H, Wang S, Humphries CG, Carstens R and Huffman KE. Inhibition of cancer cell proliferation by PPARγ is mediated by a metabolic switch that increases reactive oxygen species levels. Cell Metab 2014; 20: 650-661.

[22] Morais JF, Sant'Anna JR, Pereira TS, Franco CC, Mathias PC and de Castro-Prado MA. Genotoxic investigation of a thiazolidinedione PPARγ agonist using the in vitro micronucleus test and the in vivo homozygotization assay. Mutagenesis 2016; 31: 417-424.

[23] Moon HS, Guo DD, Lee HG, Choi YJ, Kang JS, Jo K, Eom JM, Yun CH and Cho CS. Alpha-eleostearic acid suppresses proliferation of MCF-7 breast cancer cells via activation of PPARγ and inhibition of ERK 1/2. Cancer Sci 2010; 101: 396-402.

[24] Kole L, Sarkar M, Deb A and Giri B. Pioglitazone, an anti-diabetic drug requires sustained MAPK activation for its anti-tumor activity in MCF7 breast cancer cells, independent of PPAR-γ pathway. Pharmacol Rep 2016; 68: 144-154.

[25] Ching J, Amiridis S, Stylli SS, Bjorksten AR, Kountouri N, Zheng T, Paradiso L, Luwor RB, Morokoff AP and O'Brien TJ. The peroxisome proliferator activated receptor gamma agonist pioglitazone increases functional expression of the glutamate transporter excitatory amino acid transporter 2 (EAAT2) in human glioblastoma cells. Oncotarget 2015; 6: 21301.

[26] Cellai I, Petrangolini G, Tortoreto M, Pratesi G, Luciani P, Deledda C, Benvenuti S, Ricordati C, Gelmini S and Ceni E. In vivo effects of rosiglitazone in a human neuroblastoma xenograft. Br J Cancer 2010; 102: 685.

[27] Belury MA. Inhibition of carcinogenesis by conjugated linoleic acid: potential mechanisms of action. J Nutr 2002; 132: 2995-2998.

[28] Shu L, Huang R, Wu S, Chen Z, Sun K, Jiang Y and Cai X. PPARγ and its ligands: potential antitumor agents in the digestive system. Curr Stem Cell Res Ther 2016; 11: 274-281.

[29] Kota B, Huang T and Roufogalis B. An overview on biological mechanisms of PPARs. Pharmacol Res 2005; 51: 85-94.

[30] Evans RM and Mangelsdorf DJ. Nuclear receptors, RXR, and the big bang. Cell 2014; 157: 255-266.

[31] Kimball AB, Grant RA, Wang F, Osborne R and Tiesman JP. Beyond the blot: cutting edge tools for genomics, proteomics and metabolomics analyses and previous successes. Br J Dermatol 2012; 166 Suppl 2: 1-8.

[32] Foulkes AC, Watson DS, Griffiths CEM, Warren RB, Huber W and Barnes MR. Research techniques made simple: bioinformatics for genome-scale biology. J Invest Dermatol 2017; 137: e163-e168.

[33] Mele M, Ferreira PG, Reverter F, DeLuca DS, Monlong J, Sammeth M, Young TR, Goldmann JM, Pervouchine DD, Sullivan TJ, Johnson R, Segre AV, Djebali S, Niarchou A, Wright FA, Lappalainen T, Calvo M, Getz G, Dermitzakis ET, Ardlie KG and Guigo R. Human genomics. The human transcriptome across tissues and individuals. Science 2015; 348: 660-665.

[34] Irizarry R, Hobbs B, Collin F, Beazer-Barclay Y, Antonellis K, Scherf U and Speed T. Exploration, normalization, and summaries of high density oligonucleotide array probe level data. Biostatistics 2003; 4: 249-264.

[35] Szklarczyk D, Franceschini A, Wyder S, Forslund K, Heller D, Huerta-Cepas J, Simonovic M, Roth A, Santos A, Tsafou KP, Kuhn M, Bork P, Jensen LJ and von Mering C. STRING v10: protein-protein interaction networks, integrated over the tree of life. Nucleic Acids Res 2015; 43: D447-452.

[36] Lin Z and Lin Y. Identification of potential crucial genes associated with steroid-induced necrosis of femoral head based on gene expression profile. Gene 2017; 627: 322-326.

[37] Wang JH, Zhao LF, Lin P, Su XR, Chen SJ, Huang LQ, Wang HF, Zhang H, Hu ZF and Yao KT. GenCLiP 2.0: a web server for functional clustering of genes and construction of molecular networks based on free terms. Bioinformatics 2014; 30: 2534-2536.

[38] Shannon P, Markiel A, Ozier O, Baliga NS, Wang JT, Ramage D, Amin N, Schwikowski B and Ideker T. Cytoscape: a software environment for integrated models of biomolecular interaction networks. Genome Res 2003; 13: 2498-2504.

[39] Mou T, Zhu D, Wei X, Li T, Zheng D, Pu J, Guo Z and Wu Z. Identification and interaction analysis of key genes and microRNAs in hepatocellular carcinoma by bioinformatics analysis. World J Surg Oncol 2017; 15: 63.

[40] Fan Y, Zhou X, Xia T, Chen Z, Li J, Liu Q, Alolga R, Chen Y, Lai M, Li P, Zhu W and Qi L. Human plasma metabolomics for identifying differential metabolites and predicting molecular subtypes of breast cancer. Oncotarget 2016; 7: 9925-9938.

[41] Tang X, Lin CC, Spasojevic I, Iversen ES, Chi JT and Marks JR. A joint analysis of metabolomics and genetics of breast cancer. Breast Cancer Res 2014; 16: 415.

[42] Budczies J, Pfitzner BM, Györffy B, Winzer KJ, Radke C, Dietel M, Fiehn O and Denkert C. Glutamate enrichment as new diagnostic opportunity in breast cancer. Int J Cancer 2015; 136: 1619-1628.

[43] Lien EC, Lyssiotis CA, Juvekar A, Hu H, Asara JM, Cantley LC and Toker A. Glutathione biosynthesis is a metabolic vulnerability in PI (3) K/Akt-driven breast cancer. Nat Cell Biol 2016; 18: 572.

[44] Liu Z, Wang Y, Dou C, Sun L, Li Q, Wang L, Xu Q, Yang W, Liu Q and Tu K. MicroRNA-1468 promotes tumor progression by activating PPAR-γ-mediated AKT signaling in human hepatocellular carcinoma. J Exp Clin Cancer Res 2018; 37: 49.

[45] Ni J, Zhou Ll, Ding L, Zhao X, Cao H, Fan F, Li H, Lou R, Du Y and Dong S. PPARγ agonist efatutazone and gefitinib synergistically inhibit the proliferation of EGFR-TKI-resistant lung adenocarcinoma cells via the PPARγ/PTEN/Akt pathway. Exp Cell Res 2017; 361: 246-256.

[46] Burotto M and Szabo E. PPARγ in head and neck cancer prevention. Oral Oncol 2014; 50: 924-929.

[47] Halstead AM, Kapadia CD, Bolzenius J, Chu CE, Schriefer A, Wartman LD, Bowman GR and Arora VK. Bladder-cancer-associated mutations in RXRA activate peroxisome proliferator-activated receptors to drive urothelial proliferation. Elife 2017; 6.

[48] Borland MG, Kehres EM, Lee C, Wagner AL, Shannon BE, Albrecht PP, Zhu B, Gonzalez FJ and Peters JM. Inhibition of tumorigenesis by peroxisome proliferator-activated receptor (PPAR)-dependent cell cycle blocks in human skin carcinoma cells. Toxicology 2018; 404: 25-32.

[49] Park JI and Kwak JY. The role of peroxisome proliferator-activated receptors in colorectal cancer. PPAR Res 2012; 2012: 876418.